machines

MDPI

Article

Finite-Time Output Feedback Control for Electro-Hydraulic Servo Systems with Parameter Adaptation

Luyue Yin, Wenxiang Deng *, Xiaowei Yang and Jianyong Yao

School of Mechanical Engineering, Nanjing University of Science and Technology, Nanjing 210094, China; laurayin@njust.edu.cn (L.Y.); xwyang_njust@njust.edu.cn (X.Y.); yaojianyong@njust.edu.cn (J.Y.)
* Correspondence: wxdeng@njust.edu.cn; Tel.: +86-025-8431-5125

Abstract: Measurement noise, parametric uncertainties, and external disturbances broadly exist in electro-hydraulic servo systems, which terribly deteriorate the system control performance. To figure out this problem, a novel finite-time output feedback controller with parameter adaptation is proposed for electro-hydraulic servo systems in this paper. First, to avoid using noise-polluted signals and attain active disturbance compensation, a finite-time state observer is adopted to estimate unknown system states and disturbances, which attenuates the impact of measurement noise and external disturbances on tracking performance. Second, by adopting a parameter adaptive law, the parametric uncertainties in the electro-hydraulic servo system can be much lessened, which is beneficial to averting the high-gain feedback in practice. Then, integrating the backstepping framework and the super-twisting sliding mode technique, a synthesized output feedback controller is constructed to achieve high-accuracy tracking performance for electro-hydraulic servo systems. Lyapunov stability analysis demonstrates that the proposed control scheme can acquire finite-time stability. The excellent tracking performance of the designed control law is verified by comparative simulation results.

Keywords: motion control; finite time control; output feedback; parameter adaption; electro-hydraulic servo valve; modelling

Citation: Yin, L.; Deng, W.; Yang, X.; Yao, J. Finite-Time Output Feedback Control for Electro-Hydraulic Servo Systems with Parameter Adaptation. *Machines* **2021**, *9*, 214. https://doi.org/10.3390/machines9100214

Academic Editors: Zheng Chen and Litong Lyu

Received: 31 August 2021
Accepted: 22 September 2021
Published: 26 September 2021

1. Introduction

Hydraulic servo systems have been widely used in modern industry [1–5] due to their good capabilities such as high power/weight ratio, large output force, etc. However, the electro-hydraulic servo system is a sort of highly non-linear system with various model uncertainties which is mainly manifested in the non-linear pressure and flow of the valve. The model uncertainties of the electro-hydraulic servo system can be divided into parameter uncertainties and uncertain nonlinearities, such as parameter change, external disturbances, nonlinear friction and so on. These problems have always restricted the development of advanced control and the decision-making algorithms for electro-hydraulic servo systems. The modeling uncertainties will seriously deteriorate the performance of the designed controller and lead to cycle oscillations and even instability in the system [6]. With the development of the industry, there is increasingly high demanding for the control speed and accuracy of the hydraulic system. Thus, the traditional linear control methods have become more and more difficult to satisfy the demand of modern hydraulic servo systems. In order to solve the above problems, non-linear system controllers have been expanded in the past few decades, such as robust control [7], H infinity control [8–10], and adaptive control [11–13]. Among these methods, adaptive control can cope with parametric variations due to its learning ability.

The adaptive control (AC) [3] was generally used to deal with parameter uncertainties, but it had little effect on unmodeled disturbances. The adaptive robust control (ARC) in [14,15] could simultaneously solve the unmodeled disturbances and parameter uncertainties. However, ARC could only guarantee the bounded tracking performance when dealing with unmodeled disturbances. In order to solve the unknown nonlinearities that cannot be presented in the form of linear parameterization, function approximators have been researched, such as neural networks (NN) [16–19] and fuzzy systems (FS) [20–22]. However, these function approximators might bring heavy computational costs and require a considerable amount of time to achieve convergence, which was also affected by the adopted adaptive law and learning gains.

Sliding mode control can often be employed to handle bounded modeling uncertainties and to obtain asymptotic tracking performance in hydraulic systems [23]. However, the discontinuity of the control input will cause the controller chattering, which is not allowed for the actual hydraulic systems. In order to eliminate chattering in the sliding mode control, a continuous saturation function instead of a discontinuous sign function was used in [24], but it could only ensure bounded tracking performance [25]. The high-order sliding mode controller designed in [26] could obtain asymptotic tracking while ensuring the continuity of the controller. However, the designing process of the controller required the derivative of the sliding mode, which was difficult to implement in engineering. Super-twisting sliding mode control in [27,28] could not only retain the high robustness, but also solve the high frequency chattering problem. Additionally, as the second-order sliding mode algorithm, the super-twisting sliding mode control could also obtain finite-time stability. In 2006, a review article in a book by Dorato explained the strong robustness of finite-time stability [29], which pointed out the difference between finite-time stability and the stability under traditional concepts. In the meanwhile, the superiority of this method in transient response performance was proved. Based on this method, many results have been achieved [30–35]. Unfortunately, none of the above controllers have considered the uncertainties of the system parameters. In [36], some researchers proposed the finite time control with parameter adaptation. However, most of them were for linear systems. An adaptive finite-time controller for nonlinear systems with parametric uncertainties was proposed in [37]. This controller based on backstepping methodology could not only realize the finite-time stability in the nonlinear system, but also synthesize the advantages of parameter adaptation. Nevertheless, the condition that all system states in the above-mentioned literature need to be known, is not easy to be satisfied in practice.

Backstepping methodology is used in most of the existing electro-hydraulic system control [38]. In these backstepping designs, the entire system state must be known or measurable due to the strict backstepping process. However, the velocity and acceleration signals in hydraulic systems are usually unmeasurable due to lack of sensors. Though they can be acquired by numerical differentiation on the position measurement, the obtained velocity and acceleration signals are accompanied by strong measurement noise. Therefore, in order to avoid using these variables in the control design, some output feedback controllers that only uses measurable output for practical application have been developed. In [39], an output feedback controller based on extend state observer was proposed to estimate the unmeasurable state variables through output variables, but it could only guarantee global uniformly ultimately bounded tracking performance. In [40], an output feedback control based on a finite-time observer was proposed, but it did not consider parameter adaptation. In [41], Levant proposed an output-feedback controller based on a higher-order sliding mode differentiation. Compared with the extended state observer, the finite-time observer has better transient response performance.

Motivated by the above observations, the following problems are expected to be resolved in this paper: (1) avoid using the noise-contaminated velocity and acceleration signals in the control design; (2) eliminate the high-gain feedback issue in the existing sliding mode control methods; and (3) achieve the excellent finite-time tracking performance with zero steady-state error for the electro-hydraulic servo system. Therefore, a finite-time output feedback controller with parameter adaptation (FOFA) is proposed for electro-hydraulic servo systems in this paper. In order to complete this research, a nonlinear model of the electro-hydraulic servo system considering the parameter uncertainties and external disturbances is established. Aiming at the stability problem of the electro-hydraulic servo system under the condition of parameter uncertainties and system disturbances, this paper adopts a parameter adaptive law to remove the parametric uncertainties. Then integrating the backstepping framework and the super-twisting sliding mode technique, a composite output feedback controller is designed to achieve high-accuracy tracking performance for electro-hydraulic servo systems. Parameter adaptation and super-twisting sliding mode are combined in an innovative way, and feedforward compensation is performed through parameter adaptation, which can effectively prevent system instability caused by high-gain feedback and achieve finite time stability. Also, an output feedback control method realized by finite-time observer is combined to achieve the estimations of unknown system states and to compensate for the unmodeled and external disturbances. Lyapunov stability analysis demonstrates that the proposed control scheme can acquire finite-time stability, and the excellent tracking performance of the designed control law is verified by comparative simulation results.

The organization structure of this paper is as follows: Section 2 presents the problem formation and dynamic model. Section 3 presents the design process and theoretical results of finite time observer and adaptive law of the finite time output feedback controller proposed in this paper. Section 4 provides the simulation settings and comparison of results. Section 5 discusses the conclusion.

2. Dynamic Model and Problem Formulation

The equipment considered in this paper is descripted in Figure 1. Our purpose is to ensure that the tracking output can track the desired trajectory as closely as possible. The dynamic equation of the inertial load of the servo system can be described as follows:

$$m\ddot{y} = A(P_1 - P_2) - B\dot{y} + L(t) \tag{1}$$

where y represents the displacement and m represents the inertial mass of load; $P_L = P_1 - P_2$ stands for the load pressure of hydraulic actuator, in which P_1 and P_2 are the pressures inside two chambers of the hydraulic cylinders, separately; A denotes the effective area of ram of the two chambers, B represents viscous friction coefficient, and $L(t)$ represents the external and unmodeled disturbances of the hydraulic cylinders.

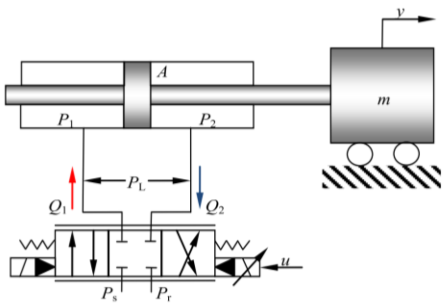

Figure 1. Schematic diagram of the hydraulic actuator system.

The load pressure dynamics can be written as

$$\frac{V_t}{4\beta_e}\dot{P}_L = -A\dot{y} - C_t P_L + Q_E + Q_L \tag{2}$$

where V_t is the total control volume of the actuator; β_e is the effective oil bulk modulus; C_t represents the internal leakage coefficient of the chambers due to pressure; Q_E is the time-varying modeling error caused by complicated internal leakage, parameter deviations, unmodeled pressure dynamics, modeling error caused by the following flow equation, and so on; $Q_L = (Q_1 + Q_2)/2$ is the load flow; Q_1 is the supplied flow rate to the forward chamber; and Q_2 is the return flow rate of the return chamber. According to [4], Q_L is related to the spool valve displacement of the servo valve, and it can be deduced that

$$Q_L = k_q x_v \sqrt{P_s - sign(x_v)P_L} \tag{3}$$

where $k_q = C_d w\sqrt{1/\tau}$ represents the flow rate gain, C_d is the discharge coefficient; x_v is the spool valve displacement of the servo valve; P_s is the supply pressure of the fluid with respect to the return pressure P_r; and $sign\ (\cdot)$ denotes the standard signum function as

$$sign(x_v) = \begin{cases} 1 \text{ if } x_v > 0 \\ 0 \text{ if } x_v = 0 \\ -1 \text{ if } x_v < 0 \end{cases} \tag{4}$$

The effects of servo-valve dynamics have been included by some researchers [42,43]. However, additional sensors are required to obtain the spool position, and only minimal performance improvement can be achieved for motion tracking. In addition, valve dynamics will increase the system order and complicate the controller design. Therefore, many literatures neglect servo-valve dynamics. Consequently, the control input applied to the servo-valve is supposed to be directly proportional to the spool position since a high response servo-valve is used here, i.e., $x_v = k_i u$, where k_i is a positive constant; u is the control input voltage.

The flow Equation (3) can be rewritten by

$$Q_L = k_t u \sqrt{P_S - sign(u)P_L} \tag{5}$$

where $k_t = k_i k_q$ represents the coefficient of the flow rate to the pressure of the hydraulic servo valve. $(y, \dot{y}, \ddot{y})$ represent the model states, but only y and $\dot{y}$ are necessary to be concerned. So, in this paper, the state has been delimited as: $x = [x_1, x_2, x_3]^T = [y, \dot{y}, \ddot{y}]^T$. Then the whole system is:

$$\begin{aligned} \dot{x}_1 &= x_2 \\ \dot{x}_2 &= x_3 \\ \dot{x}_3 &= f_1(u, P_L)u - f_2(x_2) - f_3(x_3) + d(t) \end{aligned} \tag{6}$$

where

$$\begin{cases} f_1(u, P_L) = \frac{4A\beta_e k_t}{mV_t}\sqrt{P_s - sig(u)P_L} \\ f_2(x_2) = \frac{4\beta_e}{mV_t}(A^2 + BC_t)x_2 \\ f_3(x_3) = \frac{4\beta_e}{V_t}C_t x_3 + \frac{B}{m}x_3 \\ d(t) = \frac{4A\beta_e}{mV_t}Q_E + \frac{1}{m}\dot{L}(t) + \frac{4\beta_e}{mV_t}C_t L(t) \end{cases} \tag{7}$$

3. Nonlinear Output Feedback Controller Design

Due to the large changes in hydraulic parameters, the system is always affected by parameter uncertainties. For example, β_e and C_t are typically influenced by temperature and component wear. Therefore, the parameter uncertainties should be estimate and compensate in the parameter adaption design. Also, the unmodeled and external disturbances should be processed and compensated in the observer design.

3.1. Design Model and Issues to Be Addressed

In order to accomplish the above missions, we first define $x_4 = d(t)$ and $H(t)$ as the derivative of x_4. Then redefine system states as $x_{ob} = [x_1, x_2, x_3, x_4]^T$. Based on Equation (6), the following equation can be obtained

$$\begin{cases} \dot{x}_1 = x_2 \\ \dot{x}_2 = x_3 \\ \dot{x}_3 = f_1(u, P_L)u - f_2(x_2) - f_3(x_3) + x_4 \\ \dot{x}_4 = H(t) \end{cases} \tag{8}$$

Define an unknown parameter vector as $\theta = [\theta_1, \theta_2, \theta_3]^T$. Utilizing these state variables, the system can be expressed as

$$\begin{aligned} \dot{x}_1 &= x_2 \\ \dot{x}_2 &= x_3 \\ \dot{x}_3 &= \theta_1 R u - \theta_2 x_2 - \theta_3 x_3 + x_4 \\ \dot{x}_4 &= H(t) \end{aligned} \tag{9}$$

where

$$\begin{cases} \theta_1 = \frac{4A\beta_e k_v}{mV_t} \\ \theta_2 = \frac{4\beta_e}{mV_t}\left(A^2 + BC_t\right) \\ \theta_3 = \frac{4\beta_e}{V_t}C_t + \frac{B}{m} \end{cases} \tag{10}$$

Some assumptions are presented before designing the controller.

Assumption 1: *The unmodeled disturbances are bounded and satisfy.*

$$\left|d(t)\right| \le \delta_1, \left|\dot{d}(t)\right| \le \delta_2, |L(t)| \le \delta_3 \tag{11}$$

in which δ_1, δ_2 and δ_3 are unknown positive constants.

Assumption 2: *$|P_L|$ is sufficiently smaller than P_s, which pledges $f_1(u, P_L)$ stays far away from zero. $f_1(u, P_L)$ is not differentiable at $u = 0$ because the function $sig(u)$ exists. However, except the singular point $u = 0$, $f_1(u, P_L)$ is always continuous in any place and differentiable in other points, its left and right derivatives at $u = 0$ exist and are bounded [14]. Thus, the following assumption is rational.*

Assumption 3: *According to Equation (1) and Assumption 1, P_L is Lipschitz in regard to x_3 and x_2, thus the functions $f_1(u, P_L)$ is Lipschitz in regard to x_3 and x_2 in its practical range, which is rewritten as $f_1(u, x_2, x_3)$; $f_2(x_2)$ and $f_3(x_3)$ are globally Lipschitz in regard to x_2 and x_3, respectively.*

Assumption 4: *The desired motion trajectory $x_{1d} \in C^3$ is bounded; In practical hydraulic systems under normal working conditions, P_1 and P_2 are always bounded by P_s and P_r, i.e., $0 \le P_r < P_1 < P_s$, $0 \le P_r < P_2 < P_s$.*

Assumption 5: *The unknown parameter set θ satisfies.*

$$\theta \in \Omega_\theta \triangleq \{\theta : \theta_{\min} \le \theta \le \theta_{\max}\} \tag{12}$$

where $\theta_{max} = [\theta_{1max}, \ldots, \theta_{3max}]^T$, $\theta_{min} = [\theta_{1min}, \ldots, \theta_{3min}]^T$ are the known upper and lower bounds.

3.2. Projection Mapping

In the following sections, $\bullet_i$ denotes the ith element of the vector $\bullet$, and the operation for two vectors is performed in terms of the corresponding elements of the vectors.

Define $\hat{\theta}$ as the estimate of θ and $\tilde{\theta} = \hat{\theta} - \theta$ as the estimation error. To ensure the stability of the adaptation law and limit the parameter estimation within the range defined in Equation (12), a discontinuous projection can be represented as [14,44]

$$\mathrm{Proj}_{\hat{\theta}_i}(\bullet_i) = \begin{cases} 0 & \text{if } \hat{\theta}_i = \theta_{i\max} \text{and } \bullet_i > 0 \\ 0 & \text{if } \hat{\theta}_i = \theta_{i\min} \text{and } \bullet_i < 0 \\ \bullet_i & \text{otherwise} \end{cases} \tag{13}$$

where $i = 1, \ldots, 3$. Then the following adaptation law is given by

$$\dot{\hat{\theta}} = \mathrm{Proj}_{\hat{\theta}}(\Gamma\tau) \quad \hat{\theta}(0) \in \Omega_\theta \tag{14}$$

In which $\mathrm{Proj}_{\hat{\theta}}(\bullet) = [\mathrm{Proj}_{\hat{\theta}_1}(\bullet_1), \ \ldots, \ \mathrm{Proj}_{\hat{\theta}_3}(\bullet_3)]^T$; $\Gamma > 0$ is a positive diagonal adaptation rate matrix; τ is an adaptation function to be synthesized later. For any adaptation function τ, the discontinuous projection used in Equation (13) satisfies [14]

$$\begin{array}{l} \hat{\theta} \in \Omega_{\hat{\theta}} = \left\{\hat{\theta} : \theta_{\min} \leq \hat{\theta} \leq \theta_{\max}\right\} \\ \tilde{\theta}^T[\Gamma^{-1}\mathrm{Proj}_{\hat{\theta}}(\Gamma\tau) - \tau] \leq 0, \ \forall\tau. \end{array} \tag{15}$$

3.3. Finite Time Observer Design

To estimate the unknown states $x_i, i = 2, 3$ in system, the following Levant's observer is used: [40]

$$\begin{array}{l} \dot{\hat{x}}_1 = -v_1 L^{\frac{1}{4}} |\hat{x}_1 - x_1|^{\frac{3}{4}} sign(\hat{x}_1 - x_1) + \hat{x}_2 \\ \dot{\hat{x}}_2 = -v_2 L^{\frac{1}{3}} \left|\hat{x}_2 - \dot{\hat{x}}_1\right|^{\frac{2}{3}} sign\left(\hat{x}_2 - \dot{\hat{x}}_1\right) + \hat{x}_3 \\ \dot{\hat{x}}_3 - \hat{\vartheta}\Phi = -v_3 L^{\frac{1}{2}} \left|\hat{x}_3 - \dot{\hat{x}}_2\right|^{\frac{1}{2}} sign\left(\hat{x}_3 - \dot{\hat{x}}_2\right) + \hat{x}_4 \\ \dot{\hat{x}}_4 = -v_4 L sign\left(\hat{x}_4 - \left(\dot{\hat{x}}_3 - \hat{\vartheta}\Phi\right)\right) \end{array} \tag{16}$$

where $\hat{x}_i (i = 1, 2, 3, 4)$ are estimations of all states and $\tilde{x}_i = \hat{x}_i - x_i$ are the estimation errors; $\Phi = [Ru, -\hat{x}_2, -\hat{x}_3]^T$, L is the Lipschitz constant in the observer, v_1, v_2, v_3, v_4 is the positive observation coefficient.

Remark 1. *If the sensor noise and the parameter adaptive estimation error in the measured output*x_1 *is bounded to* $v > 0$*; then the estimation errors of (16) will converge to a small set around zero in finite time* t_c*, i.e.,* $|\tilde{x}_i| = |\hat{x}_i - x_i| \leq \ell_i v^{(n-i+2)/(n+1)}$*,* $i = 1, \ldots, 3$ *for* $t \geq t_c > 0$ *where* ℓ_i *are positive constants determined by gains* v_1, v_2, v_3, v_4*. If the measured output* x_1 *is free from sensor noise, the observer errors will converge to zero in finite time [40].*

3.4. Controller Design

In this section, by using the estimated states and disturbance obtained from the finite time observer, the nonlinear controller is presented.

Step 1: Before designing the controller, define a set of variables as

$$\begin{cases} z_1 = x_1 - x_{1d} \\ z_2 = \dot{z}_1 + k_1 z_1 = x_2 - x_{2eq} \\ x_{2eq} = \dot{x}_{1d} - k_1 z_1 \\ z_3 = \dot{z}_2 + k_2 z_2 = x_3 - x_{3eq} \\ x_{3eq} = \dot{x}_{2eq} - k_2 z_2 \\ e_1 = \hat{x}_1 - x_{1d} \\ e_2 = \hat{x}_2 - x_{4eq} \\ x_{4eq} = \dot{x}_{1d} - k_1 e_1 \\ e_3 = \hat{x}_3 - x_{5eq} \\ x_{5eq} = \dot{x}_{4eq} - k_2 e_2 \\ \hat{x}_{3eq} = \dot{x}_{5eq} = \dddot{x}_{1d} - k_1 \ddot{\hat{x}}_1 + k_1 \ddot{x}_{1d} - k_2 \dot{\hat{x}}_2 + k_2 \ddot{x}_{1d} - k_1 k_2 \dot{\hat{x}}_1 + k_1 k_2 \dot{x}_{1d} \end{cases} \tag{17}$$

where x_{1d} is the desired displacement trajectory; k_1 and k_2 are positive; $\dot{x}_{1d}$ is the 1th derivative of; $\ddot{x}_{1d}$ is the 2th derivative of x_{1d}; z_1 is the system output tracking error; z_2 is the difference between x_2 and x_{2eq}; z_3 is the difference between x_3 and x_{3eq}; e_1 is the difference between $\hat{x}_1$ and x_{1d}; e_2 is the difference between $\hat{x}_2$ and x_{4eq}; e_3 is the difference between $\hat{x}_3$ and x_{5eq}; $\dot{e}_3$ is the 1th derivative of e_3; and $\dddot{x}_{1d}$ is the 3th derivative of x_{1d}. According to Equation (17), the following equation can be obtained:

$$\begin{cases} e_1 = z_1 + \widetilde{x}_1 \\ e_2 = z_2 + \widetilde{x}_2 + k_1\widetilde{x}_1 \\ e_3 = z_3 + \widetilde{x}_3 + M_1 + M_2 \end{cases} \tag{18}$$

where

$$M_1 = (k_1 + k_2)\widetilde{x}_2, M_2 = -k_1\lambda_1|\widetilde{x}_1|^{\frac{3}{4}}sign(\widetilde{x}_1) + k_1k_2\widetilde{x}_1 \tag{19}$$

Step 2: In order to develop the super-twisting sliding mode controller, define the sliding mode surface

$$s = c_1e_1 + c_2e_2 + e_3 \tag{20}$$

where the parameters c_1 and c_2 are Hurwitz and positive.

Therefore, based on Equations (6), (14), (18) and (20), the form of the control input u is expressed by

$$\begin{cases} u = \frac{\hat{\theta}_2\hat{x}_2+\hat{\theta}_3\hat{x}_3-\hat{x}_4-c_1\dot{e}_1-c_2\dot{e}_2+\dot{\hat{x}}_{3eq}+u_n-\beta_1 sign(s)|s|^{\frac{1}{2}}}{\hat{\theta}_1 R} \\ \dot{u}_n = -\beta_2 sign(s)/2 \end{cases} \tag{21}$$

According to Equations (6), (9), (16), (18) and (20), the dynamic of s is expressed as

$$\begin{cases} \dot{s} = u_n - \beta_1 sign(s)|s|^{\frac{1}{2}} + \varphi(\widetilde{x}_1, \widetilde{x}_2, \widetilde{x}_3, \widetilde{x}_4) - \widetilde{\theta}^T\Phi \\ \dot{u}_n = -\beta_2 sign(s) \end{cases} \tag{22}$$

where

$$\varphi(\widetilde{x}_1, \widetilde{x}_2, \widetilde{x}_3, \widetilde{x}_4) = -\widetilde{x}_4 + \widetilde{\dot{x}}_{3eq} + \dot{\widetilde{x}}_3 + \dot{M}_1 + \dot{M}_2 \tag{23}$$

$$M_1 = (k_1 + k_2)\widetilde{x}_2, M_2 = -k_1v_1|\widetilde{x}_1|^{\frac{3}{4}}sign(\widetilde{x}_1) + k_1k_2\widetilde{x}_1 \tag{24}$$

According to the results of Remark 1, it can be inferred that $|\varphi(\widetilde{x}_1, \widetilde{x}_2, \widetilde{x}_3, \widetilde{x}_4)| \leq \rho$, in which ρ is a bounded constant.

3.5. Main Results

Theorem 1. *Based on Assumption 1~5, the Equations (21) and (22), and satisfying the following conditions:*

(1) $\beta_1 > \frac{[4\varepsilon^2+\lambda+2\varepsilon\rho]^2}{8\varepsilon\lambda} + \frac{\rho(4\varepsilon^2+\lambda)}{2\lambda}$
(2) $\beta_2 = 2\varepsilon\beta_1$
(3) $\tau = \Phi[\chi_1(\lambda + 4\varepsilon^2) - 4\chi_2\varepsilon]$

Then it can be guaranteed that there exists $0 < T_0 \leq 2\sqrt{V(t_0)}/r$ such that the sliding mode surface s converges to an arbitrary small region around zero, in which β_1, β_2, λ and ε are all arbitrary positive constants [23].

Proof of Theorem 1. See Appendix A. □

Remark 2. *The result of Theorem 1 shows that the proposed finite-time output feedback controller with parameter adaption has finite-time convergence performance. This method ensuring transient performance and final tracking accuracy is very important for precise motion control of hydraulic systems.*

4. Simulation Results and Discussion

In order to verify the dynamic tracking performance of the controller proposed in this paper, linear output feedback control with parameter adaptation (LOFC) and PID control method are compared separately.

The simulation model parameters of hydraulic manipulation system are chosen as follows: P_s = 7 MPa, P_r = 0 MPa, $A_1 = A_2 = A$ = 2 × 10^{-4} m^2, V_t = 2 × 10^{-3} m^3, m = 40 kg, β = 200 MPa, C_t = 7 × 10^{-12} m^5/N/s, $k_t = 9.25 \times 10^{-8}$ m$^4/(s \cdot V \cdot \sqrt{N})$. The initial estimates of θ are chosen as $\hat{\theta}_0 = [0.1,\ 200,\ 1]$. The bounds of θ are chosen as $\theta_{\max}$ = [10, 1 × 10^4, 100]$^{\mathrm{T}}$, $\theta_{\min}$ = [−1, 100, −10]$^{\mathrm{T}}$. The simulation step size is set to 0.5ms and the applied disturbance is $d(t)$ = 2sin(t). The following three controllers are compared:

(1) **FOFA:** This is the finite-time output feedback controller with parameter adaptation proposed in this paper. The following control gains are utilized: k_1 = 120, k_2 = 700. Γ = diag{8, 1 × 10^8, 1 × 10^7}, L = 5000, β = 10, ε = 1 × 10^{-4}, λ = 1 × 10^{-3}.

(2) **LOFC:** To compare with the FOFA control method, an ESO based linear output feedback control with parameter adaptation controller has been adopted. Linear feedback control and parameter adaption have been applied to this output feedback controller based ESO. The desired compensation of the controller is also solved via observer estimation and parameter adaption, similar to FOFA. The LOFC controller is utilized as $u = -\frac{1}{\hat{\theta}_1}\left(\hat{\theta}_2\varphi_2 + \hat{\theta}_3\varphi_3 - \dot{x}_{5eq}\right) - k_L e_3 - \hat{x}_4$, where k_L is positive constant. The gains of the linear output feedback control with parameter adaptation controller is Γ = diag{2, 3920, 200}, k_1 = 8, k_2 = 5, k_L = 5.

(3) **PID:** To compare with the traditional control method, Proportional-Integral-Derivative (PID) controller is utilized as $u = k_p(x_{1d} - x_1) + k_i\int_0^t (x_{1d} - x_1)dt + k_d\frac{d(x_{1d}-x_1)}{dt}$ in this servo system. The control parameters are selected as k_p = 4000, k_i = 2000, k_d = 4500.

4.1. Comparison and Analysis of Sine Tracking Performance

In order to further verify the dynamic tracking performance of the proposed FOFA controller, the desired curve was designed as sine curve with two different frequency conditions.

Case 1. The desired tracking command and the tracking result of FOFA is shown in Figure 2, namely, 0.5sin(πt)·(1−e$^{-0.05t}$) rad. The simulation results are shown in Figures 2–5.

The estimation of the unknown system parameters of the FOFA controller is shown in Figure 3. It can be seen that the estimations of the parameters θ_1, θ_2 and θ_3 have converged effectively. In Figure 4, it can be seen that the estimated position value and actual position value are consistent well in (a), and the estimated values of the signal x_2 and x_3 and the unmodeled disturbances can also be accurately obtained in (b) and (c), which proves the effectiveness of the observer. The unmodeled disturbance term estimated by the observer is shown in (d). As shown in Figures 2 and 5, the FOFA controller shows excellent tracking performance, and the magnitude of its steady-state tracking error is about 3 × 10^{-4} m at the maximum at the beginning and quickly converges to about 2.1 × 10^{-5} m. It can be seen that the tracking error of the FOFA controller is relatively large at the initial stage, but under the action of the parameter adaptation law and the finite time control, the estimated values of the unknown parameters of the system gradually converge, and the tracking error gradually decreases, which verifies the asymptotic tracking performance of the FOFA controller. In comparison, the amplitude of the steady-state tracking error of the LOFC controller is basically stable at about 3.5 × 10^{-4} m. The tracking error of the PID controller is maintained at about 4.9 × 10^{-4} m. Due to the large gain selected for the PID controller, the tracking error of PID controller produces slight chattering, which is not conducive to the stable operation of the actual system.

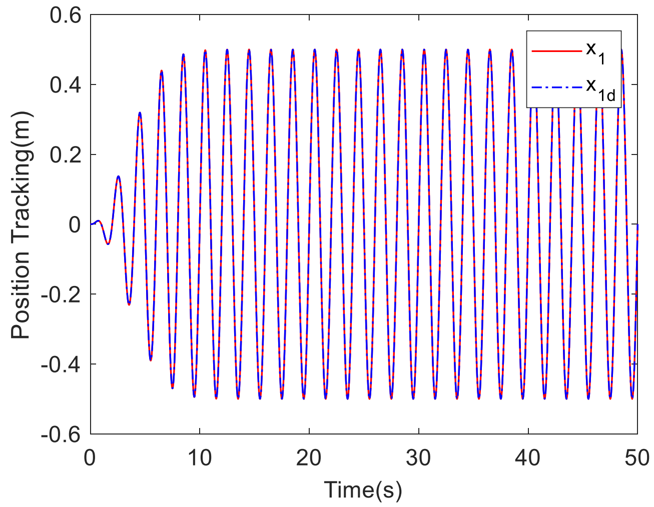

Figure 2. Tracking result of FOFA.

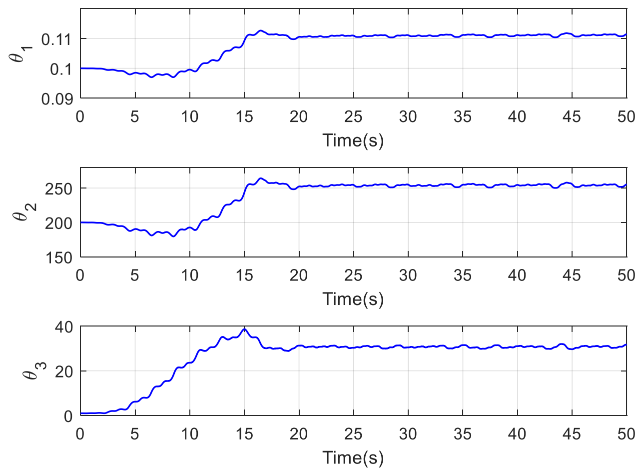

Figure 3. Parameter adaptation of FOFA.

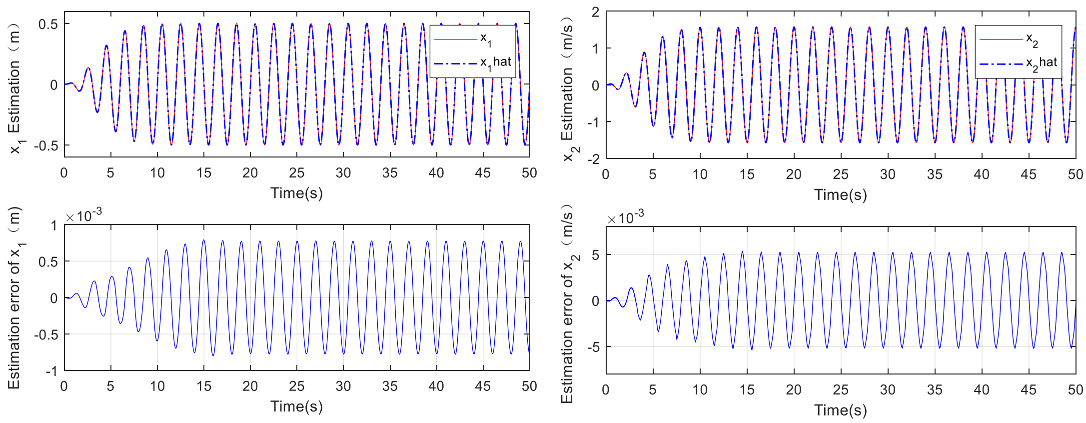

(**a**) Estimation result and error of x_1 (**b**) Estimation result and error of x_2

Figure 4. *Cont.*

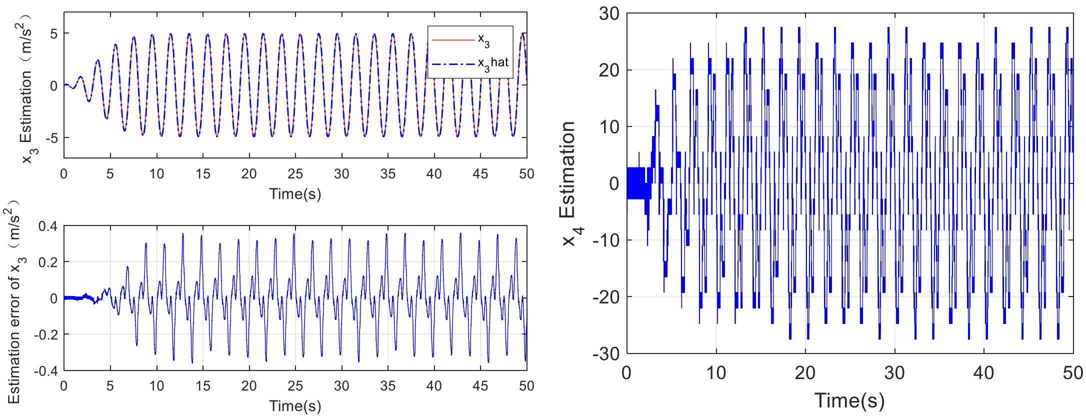

(**c**) Estimation result and error of x_3 (**d**) Estimation result of x_4

Figure 4. Estimation results of finite time observer.

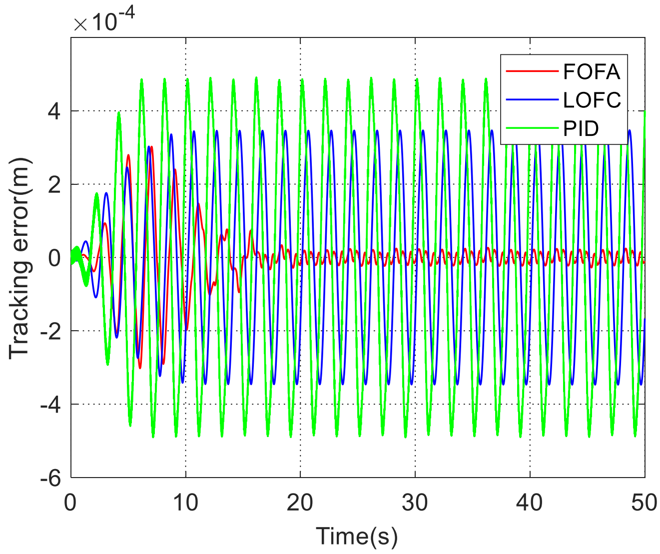

Figure 5. Comparison of position tracking error.

Case 2. The desired tracking command and the tracking result of FOFA is shown in Figure 6, namely $0.5\sin(0.5 \times \pi t)\cdot(1-e^{-0.05t})$ m.

As shown in Figures 6 and 7, the FOFA controller shows superior tracking performance, and the magnitude of its tracking error is about 1.4×10^{-4} m at the maximum at the beginning and quickly converges to about 3.1×10^{-5} m. In comparison, the magnitude of tracking error of LOFC is about 2.43×10^{-4} m at the maximum, and the amplitude of the steady-state tracking error of the LOFC controller in is stable at about 1.02×10^{-4} m. The tracking error of the PID controller in is maintained at about 5.28×10^{-4} m.

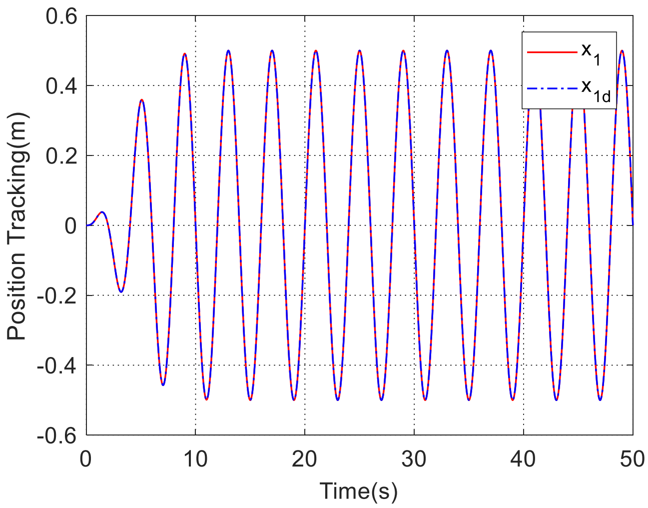

Figure 6. Tracking result of FOFA.

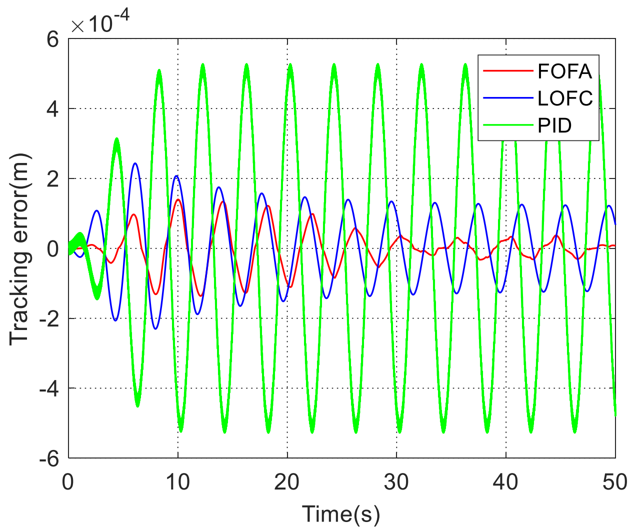

Figure 7. Comparison of position tracking error.

4.2. Comparison and Analysis of Point to Point Curve Tracking Performance

In order to further verify the tracking performance of the FOFA controller proposed in this paper, the desired tracking command is designed as point to point curve. the desired tracking command and the tracking result of FOFA are shown in Figure 8. The simulation results are shown in Figures 8 and 9.

Figure 8 shows the tracking process and tracking error of the of the FOFA controller. Due to a sudden change in the expected instruction, it can be seen that the tracking error of the FOFA controller is about -3.6×10^{-5} m at the maximum, which is relatively large at the initial stage. The final tracking error stabilizes at 2.9×10^{-6} m. The tracking error of the LOFC controller is about -3.9×10^{-4} m at the maximum and the final tracking error of LOFC stabilizes at 6.7×10^{-5} m. It can be seen that slight chattering with an amplitude about 4×10^{-5} m is obtained in the final steady state by PID controller, due to the high-gain feedback selected, which is not conducive to the stable operation of the actual system. The LOFC controller takes advantage of the robustness of linear feedback control, and parameter adaptation that can estimate and compensate unknown system parameters, as well as Extended-State-Observer that attains feed-forward compensation for unmodeled and external disturbances in the system. Therefore, the transient and steady-state tracking performance of the LOFC controller is much better than the PID controller. The finite time control method combined with parameter adaption in FOFA controller can ensure that the system tracking error achieves finite time convergence through the analysis of Lyapunov function. While the control method used in LOFC controller is linear feedback method, which can only ensure that the system tracking error achieves a bounded stability. Therefore, the robustness of FOFA controller is stronger than that of LOFC controller. In addition, the finite time observer can achieve finite time convergence, while the ESO can only achieve exponential convergence, so the observation performance of the finite time observer is better than ESO. From Figure 9, it can be seen that although both controllers use parameter adaptation for feedforward compensation, the tracking performance of the FOFA controller is better than that of the LOFC controller.

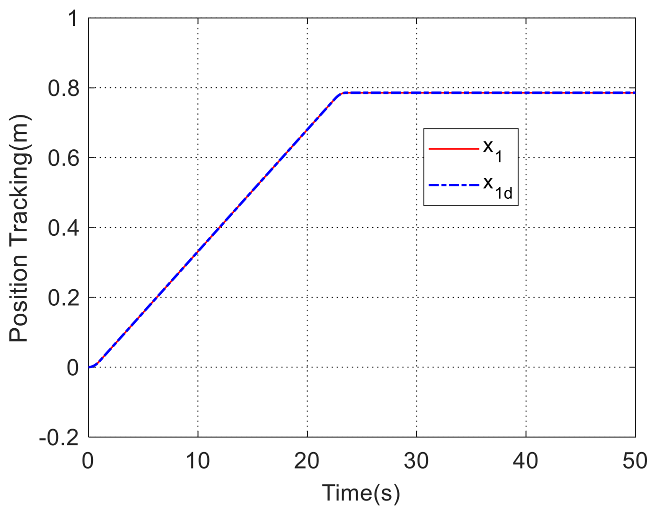

Figure 8. Tracking result of FOFA.

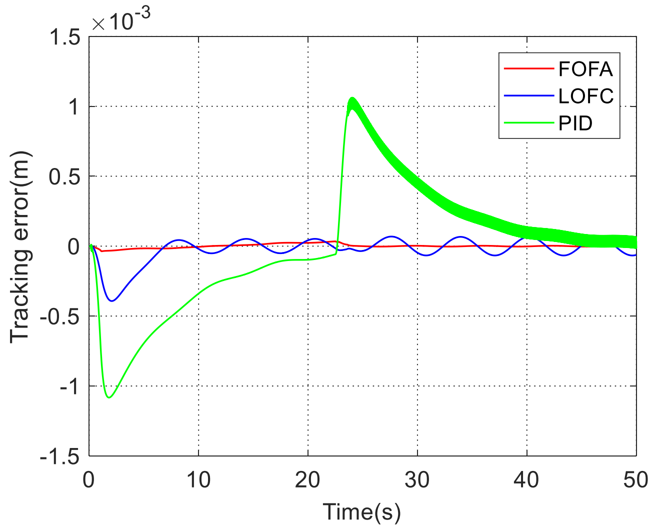

Figure 9. Comparison of position tracking error.

5. Conclusions

In this paper, a finite-time output feedback control with parameter adaptation is proposed for hydraulic servo system. This control strategy takes into account the non-measured states, parametric uncertainties and unmodeled disturbances. Based on the output position signal, the finite-time Levant observer is first employed to estimate the unmeasured states and unmodeled disturbances, which can eliminate the impact of measurement noise and disturbances on control performance in a finite time. Then, based on a parameter adaptive law, the parametric uncertainties in the system can be much relieved, which can effectively reduce the high-gain feedback. In addition, in order to suppress the residual error of disturbances and further achieve excellent transient and steady-state tracking performance, a finite time output feedback super-twisting sliding mode controller has been presented. Through the stability analysis based on Lyapunov theory, it can be concluded that the developed controller has the finite-time stability. The comparative simulation results verify the effectiveness of the proposed control strategy. However, the proposed control method was only verified via numerical simulation. In the future, it is of great significance to further verify and testify the advantages of this new controller in practical experimental platform.

Author Contributions: Formal analysis, L.Y. and X.Y.; investigation, W.D.; methodology, L.Y. and W.D.; project administration, W.D. and J.Y.; writing—original draft, L.Y. All authors have read and agreed to the published version of the manuscript.

Funding: This research was supported in part by the National Natural Science Foundation of China (51905271, 52075262), in part by the Natural Science Foundation of Jiangsu Province (BK20190459) and in part by the Fundamental Research Funds for the Central Universities (30920041101).

Institutional Review Board Statement: Not applicable.

Informed Consent Statement: Not applicable.

Data Availability Statement: Not applicable.

Conflicts of Interest: The authors declare no conflict of interest.

Nomenclature

m	Inertial mass of load
x_d, y	Desired and actual displacement of the cylinders
P_1, P_2	Pressures inside two chambers of the hydraulic cylinders
P_L	Load pressure of hydraulic actuator
A	Effective area of ram of the two chambers
$L(t)$	External and unmodeled disturbances
V_t	Volume of the actuator
β_e	Effective oil bulk modulus
C_t	Internal leakage coefficient
Q_E	Time-varying modeling error
Q_1, Q_2	Supplied flow rate and return flow rate
Q_L	Load flow
C_d	Discharge coefficient
w	Spool valve area gradient
τ	Density of oil
P_s, P_r	Supply pressure and return pressure
x_v, u	Spool valve displacement and control input voltage
k_q	Flow rate gain
k_t	Coefficient of the flow rate

Appendix A

Proof of Theorem 1

According to Equation (22), define a new state vector

$$\chi = [\chi_1, \chi_2]^T = \left[sign(s)|s|^{\frac{1}{2}}, u_n\right]^T \tag{A1}$$

Then

$$\dot{\chi} = A\chi + \psi + W \tag{A2}$$

where $A = \frac{1}{2|\chi_1|}\begin{bmatrix} -\beta_1 & 1 \\ -\beta_2 & 0 \end{bmatrix}$ is Hurwitz; $\psi = \begin{bmatrix} \varphi/2|\chi_1| \\ 0 \end{bmatrix}$ $W = \begin{bmatrix} \widetilde{\vartheta}^T\Phi \\ 0 \end{bmatrix}$.

A Lyapunov function is expressed by

$$V = \frac{1}{2}\chi^T P_1 \chi + \frac{1}{2}\widetilde{\vartheta}^T \Gamma^{-1} \widetilde{\vartheta} \tag{A3}$$

$$V_o = \frac{1}{2}\chi^T P_1 \chi \tag{A4}$$

where P_1 and Γ is a positive definite matrix.

$$P_1 = \begin{bmatrix} \lambda + 4\varepsilon^2 & -2\varepsilon \\ -2\varepsilon & 1 \end{bmatrix} \tag{A5}$$

First, the derivative of V is written as follows

$$\begin{aligned} \dot{V} &= \tfrac{1}{2}\left(\dot{\chi}^T P_1 \chi + \chi^T P_1 \dot{\chi}\right) + \widetilde{\vartheta}^T \Gamma^{-1} \dot{\hat{\vartheta}} = \chi^T P_1 (A\chi + \psi - W) + \widetilde{\vartheta}^T \Gamma^{-1} \dot{\hat{\vartheta}} \\ &= 2\chi^T P_1 (A\chi + \psi) - 2\chi^T P_1 \begin{bmatrix} \widetilde{\vartheta}^T \Phi \\ 0 \end{bmatrix} + \widetilde{\vartheta}^T \Gamma^{-1} \dot{\hat{\vartheta}} \\ &\leq -\tfrac{\chi^T Q \chi}{2|\chi_1|} - 2\chi^T P_1 \begin{bmatrix} \widetilde{\vartheta}^T \Phi \\ 0 \end{bmatrix} + \widetilde{\vartheta}^T \Gamma^{-1} \dot{\hat{\vartheta}} \end{aligned} \tag{A6}$$

where the symmetric matrix $Q = \begin{bmatrix} Q_{11} & Q_{12} \\ Q_{21} & Q_{22} \end{bmatrix}$ with

$$\begin{cases} Q_{11} = 2(\beta_1 - \rho)(4\varepsilon^2 + \lambda_2) - 4\varepsilon\beta_2 \\ Q_{12} = Q_{21} = \beta_2 - (4\varepsilon^2 + \lambda_2) - 2\varepsilon(\beta_1 + \rho) \\ Q_{22} = 4\varepsilon \end{cases} \tag{A7}$$

Considering the minimal eigenvalue of Q satisfies $\lambda_{\min}(Q) \geq 2\varepsilon$, then [23]

$$\begin{cases} \beta_1 > \frac{\left[4\varepsilon^2 + \lambda + 2\varepsilon\rho\right]^2}{8\varepsilon\lambda} + \frac{\rho\left(4\varepsilon^2 + \lambda\right)}{2\lambda} \\ \beta_2 = 2\varepsilon\beta_1 \end{cases} \tag{A8}$$

where β_1, β_2, λ and ε are all arbitrary positive constants.

According to Equations (A6)–(A8), it can be acquired that

$$\dot{V}_o \leq -\frac{\lambda_{\min}(Q)\|\chi\|^2}{2|\chi_1|} \tag{A9}$$

Noting that

$$\lambda_{\min}(P_1)\|\chi\|^2 \leq V_o \leq \lambda_{\max}(P_1)\|\chi\|^2 \tag{A10}$$

$$|\chi_1| \leq \|\chi\| \leq \sqrt{\frac{V_o}{\lambda_{\min}(P_1)}} \tag{A11}$$

Then Equation (A9) can be converted into the following form:

$$\dot{V}_o \leq -r\sqrt{V_o} \tag{A12}$$

where $r = \lambda_{\min}^{1/2}(P_1)\lambda_{\min}(Q)/2\lambda_{\max}(P_1)$. The derivative of V is rewritten as

$$V \leq -r\sqrt{V_o} - 2\chi^T P_1 \begin{bmatrix} \widetilde{\vartheta}^T \Phi \\ 0 \end{bmatrix} + \widetilde{\vartheta}^T \Gamma^{-1} \dot{\hat{\vartheta}} \tag{A13}$$

The adaption law can be obtained as follow:

$$\dot{\hat{\vartheta}} = \Gamma\Phi\left[\chi_1\left(\lambda + 4\varepsilon^2\right) - 4\chi_2\varepsilon\right] \tag{A14}$$

Then Equation (A6) can be rewritten as follows by substituting Equation (A14) into Equation (A13):

$$\dot{V} \leq -r\sqrt{V} \tag{A15}$$

According to [32], the controller can converge in finite time $T_0 \leq 2\sqrt{V(t_0)}/r$. Theorem 1 is proven. □

References

1. Yao, J.; Deng, W. Active disturbance rejection adaptive control of hydraulic servo systems. *IEEE Trans. Ind. Electron.* **2017**, *64*, 6469–6477. [CrossRef]
2. Deng, W.; Yao, J.; Wang, Y.; Yang, X.; Chen, J. Output feedback backstepping control of hydraulic actuators with valve dynamics compensation. *Mech. Syst. Signal Process.* **2021**, *158*, 107769. [CrossRef]
3. Deng, W.; Yao, J. Extended-state-observer-based adaptive control of electrohydraulic servomechanisms without velocity measurement. *IEEE/ASME Trans. Mechatron.* **2020**, *25*, 1151–1161. [CrossRef]
4. Merritt, H.E. *Hydraulic Control Systems*; Wiley: New York, NY, USA, 1967.
5. Lyu, L.; Chen, Z.; Yao, B. Advanced Valves and Pump Coordinated Hydraulic Control Design to Simultaneously Achieve High Accuracy and High Efficiency. *IEEE Trans. Control Syst. Technol.* **2021**, *29*, 236–248. [CrossRef]
6. Yao, J.; Deng, W.; Sun, W. Precision Motion Control for Electro-Hydraulic Servo Systems with Noise Alleviation: A Desired Compensation Adaptive Approach. *IEEE/ASME Trans. Mechatron.* **2017**, *22*, 1859–1868. [CrossRef]
7. Plummer, A.R.; Vaughan, N.D. Robust Adaptive Control for Hydraulic Servosystems. *J. Dyn. Syst. Meas. Control* **1996**, *118*, 237–244. [CrossRef]
8. Milić, V.; Šitum, Ž.; Essert, M. Robust position control synthesis of an electro-hydraulic servo system. *ISA Trans.* **2010**, *49*, 535–542. [CrossRef]
9. Sun, W.; Gao, H.; Kaynak, O. Finite Frequency Control for Vehicle Active Suspension Systems. *IEEE Trans. Control Syst. Technol.* **2011**, *19*, 416–422. [CrossRef]
10. Chen, H.; Liu, J.; Chen, G. Application of H∞ algorithm in hydraulic control system of loader. *Int. Rev. Comput. Softw.* **2011**, *6*, 1334–1338.
11. Yao, J.; Deng, W.; Jiao, Z. RISE-Based Adaptive Control of Hydraulic Systems with Asymptotic Tracking. *IEEE Trans. Autom. Sci. Eng.* **2015**, *14*, 1–8. [CrossRef]
12. Yao, J.; Jiao, Z.; Ma, D. Adaptive Robust Control of DC Motors with Extended State Observer. *IEEE Trans. Ind. Electron.* **2014**, *61*, 3630–3637. [CrossRef]
13. Chen, Z.; Yao, B.; Wang, Q. Adaptive Robust Precision Motion Control of Linear Motors with Integrated Compensation of Nonlinearities and Bearing Flexible Modes. *IEEE Trans. Ind. Inform.* **2013**, *9*, 965–973. [CrossRef]
14. Yao, B. Desired Compensation Adaptive Robust Control. *J. Dyn. Syst. Meas. Control* **2009**, *131*, 636–650. [CrossRef]
15. Yao, B.; Al-Majed, M. High-performance robust motion control of machine tools: An adaptive robust control approach and comparative experiments. *IEEE/ASME Trans. Mechatron.* **1997**, *2*, 63–76.
16. Na, J.; Chen, Q.; Ren, X.; Guo, Y. Adaptive Prescribed Performance Motion Control of Servo Mechanisms with Friction Compensation. *IEEE Trans. Ind. Electron.* **2013**, *61*, 486–494. [CrossRef]
17. Xu, B.; Yang, C.; Shi, Z. Reinforcement Learning Output Feedback NN Control Using Deterministic Learning Technique. *IEEE Trans. Neural Netw. Learn. Syst.* **2014**, *25*, 635–641.
18. Dahunsi, O.A.; Pedro, J.O.; Nyandoro, O.T. Neural network-based model predictive control of a servo-hydraulic vehicle suspension system. *Int. J. Appl. Math. Comput. Sci.* **2009**, 1–6.
19. Liu, Y.; Huang, P.; Zhang, F.; Zhao, Y. Distributed formation control using artificial potentials and neural network for constrained multiagent systems. *IEEE Trans. Control Syst. Technol.* **2020**, *28*, 697–704. [CrossRef]
20. Cerman, O.; Husek, P. Adaptive fuzzy sliding mode control for electro-hydraulic servo mechanism. *Expert Syst. Appl.* **2012**, *39*, 10269–10277. [CrossRef]
21. Ho, T.H.; Ahn, K. Speed Control of a Hydraulic Pressure Coupling Drive Using an Adaptive Fuzzy Sliding-Mode Control. *IEEE/ASME Trans. Mechatron.* **2012**, *17*, 976–986. [CrossRef]
22. Yin, S.; Shi, P.; Yang, H. Adaptive fuzzy control of strict-feedback nonlinear time-delay systems with unmodeled dynamics. *IEEE Trans. Cybern.* **2016**, *46*, 1926–1938. [CrossRef]
23. Yang, X.; Yao, J.; Deng, W. Output feedback adaptive super-twisting sliding mode control of hydraulic systems with disturbance compensation. *ISA Trans.* **2021**, *109*, 175–185. [CrossRef]
24. Burton, J.A.; Zinober, A.S.I. Continuous approximation of vsc. *Int. J. Syst. Sci.* **1986**, *17*, 875–885. [CrossRef]
25. Boiko, I.; Fridman, L.; Pisano, A.; Usai, E. A comprehensive analysis of chattering in second order sliding mode control systems. In *Modern Sliding Mode Control Theory*; Sringer: Berlin/Heidelberg, Germany, 2008.
26. Levant, A. Homogeneity approach to high-order sliding mode design. *Automatica* **2005**, *41*, 823–830. [CrossRef]
27. Levant, A. Sliding order and sliding accuracy in sliding mode control. *Int. J. Control* **1993**, *58*, 1247–1263. [CrossRef]
28. Shtessel, Y.; Taleb, M.; Plestan, F. A novel adaptive-gain supertwisting sliding mode controller: Methodology and application. *Automatica* **2012**, *48*, 759–769. [CrossRef]

29. Dorato, P. An Overview of Finite-Time Stability. In *Current Trends in Nonlinear Systems and Control*; Birkhäuser Boston: New York, NY, USA, 2006.
30. Giorgio, B.; Alessandro, P.; Elisabetta, P.; Elio, U. A survey of applications of second-order sliding mode control to mechanical systems. *Int. J. Control* **2003**, *76*, 875–892.
31. Liu, Y.; Zhang, F.; Huang, P.; Lu, Y. Fixed-time consensus tracking for second-order multiagent systems under disturbance. *IEEE Trans. Syst. Man Cybern. Syst.* **2021**, *51*, 4883–4894. [CrossRef]
32. Utkin, V. On convergence time and disturbance rejection of super-twisting control. *IEEE Trans. Autom. Control* **2013**, *58*, 2013–2017. [CrossRef]
33. Jinpeng, Y.; Peng, S.; Lin, Z. Finite-time command filtered backstepping control for a class of nonlinear systems. *Automatica* **2018**, *92*, 173–180.
34. Levant, A. Robust exact differentiation via sliding mode technique. *Automatica* **1998**, *34*, 379–384. [CrossRef]
35. Shtessel, Y.B.; Shkolnikov, I.A.; Levant, A. Smooth second-order sliding modes: Missile guidance application. *Automatica* **2007**, *43*, 1470–1476. [CrossRef]
36. Feng, J.E.; Wu, Z.; Sun, J.B. Finite-time Control of Linear Singular Systems with Parametric Uncertainties and Disturbances. *Acta Autom. Sin.* **2005**, *31*, 634–637.
37. Hong, Y.; Wang, J.; Cheng, D. Adaptive finite-time control of nonlinear systems with parametric uncertainty. *IEEE Trans. Autom. Control* **2006**, *51*, 858–862. [CrossRef]
38. Yip, P.P.; Hedrick, J.K. Adaptive dynamic surface control: A simplified algorithm for adaptive backstepping control of nonlinear systems. *Int. J. Control* **1998**, *71*, 959–979. [CrossRef]
39. Deng, W.; Yao, J.; Ma, D. Time varying input delay compensation for nonlinear systems with additive disturbance: An output feedback approach. *Int. J. Robust Nonlinear Control* **2018**, *28*, 31–52. [CrossRef]
40. Na, J.; Li, Y.; Huang, Y.; Gao, G.; Chen, Q. Output feedback control of uncertain hydraulic servo systems. *IEEE Trans. Ind. Electron.* **2020**, *67*, 490–500. [CrossRef]
41. Levant, A. Higher-order sliding modes, differentiation and output-feedback control. *Int. J. Control* **2003**, *76*, 924–941. [CrossRef]
42. Yao, Z.; Yao, J.; Sun, W. Adaptive rise control of hydraulic systems with multilayer neural-networks. *IEEE Trans. Ind. Electron.* **2019**, *66*, 8638–8647. [CrossRef]
43. Yao, B.; Bu, F.; Chiu, G.T.C. Non-linear adaptive robust control of electro-hydraulic systems driven by double-rod actuators. *Int. J. Control* **2001**, *74*, 761–775. [CrossRef]
44. Deng, W.; Yao, J. Asymptotic tracking control of mechanical servosystems with mismatched uncertainties. *IEEE/ASME Trans. Mechatron.* **2021**, *26*, 2204–2214. [CrossRef]